Direct Parametric Reconstruction for Dynamic [^{18}F]-FDG PET/CT Imaging in the Body

Fotis A. Kotasidis, *Member IEEE* , Julian C. Matthews, *Member IEEE*, Andrew J Reader, Georgios I. Angelis, Patricia M. Price, Habib Zaidi, *Senior Member, IEEE*

Abstract— **Abdominal and thoracic [^{18}F]FDG PET/CT imaging is routinely used in clinical practice and drug development but parametric imaging based on full kinetic analysis is rarely used due to noise induced bias and variance in kinetic parameters and analysis is usually restricted to semi-quantitative indices. Direct parametric estimation using 4D image reconstruction can potentially provide parametric maps of reduced bias and variance but little or no evaluation has been done in the body. Previous studies have demonstrated that body [^{18}F]FDG PET/CT imaging can benefit from these methods but analysis was restricted to macroparameters of interest. In work, we implement and apply a recently proposed direct 4-D algorithm using a 2 tissue compartment model on simulated and real oncology [^{18}F]FDG PET/CT data to directly estimate microparameters of interest and assess potential improvements over the traditional post-reconstruction kinetic analysis. Results on the simulated data suggest clear reduction in bias for K_1, k_2 and blood volume and less for k_3. Similarly, variance reduction was observed for K_1, k_2, k_3 and K_i and less for blood volume. Evaluation on patient data demonstrated similar improvements using the direct 4-D method in agreement with simulations.**

***Index Terms*— 4-D image reconstruction, kinetic modelling, dynamic FDG imaging**

I. Introduction

KINETIC parameter estimation in dynamic PET and potential improvements in their accuracy and precision has been the subject of many investigations over the last few years with an ever increasing list of algorithms for direct parametric estimation using spatiotemporal image reconstruction [1]. Although FDG studies account for a large percentage of PET/CT scans in the body, little has been done so far to evaluate potential benefits from advanced 4D image reconstruction methods, with most studies focusing on neuroreceptor brain imaging [2]. Usually FDG PET/CT studies in the body rely on estimating simplified indices such as SUV but a lot more information can be extracted by performing full kinetic analysis. Reconstructed images in the body generally tend to be noisier compared to brain images, thus making the generation of parametric images an even more difficult task when using post reconstruction kinetic analysis. As such, estimating kinetic parameters within a direct 4D image reconstruction algorithm can potential provide improvements in parametric images, similar to those demonstrated in the brain, thus enabling parametric imaging of dynamic [^{18}F]FDG PET/CT imaging in the body to be used in clinical practice, enabling enhanced lesion detection. Previous studies have shown enhanced performance when using 4D methods, but have focused on directly estimating macroparameters of interest using simplified graphical methods such as Patlak analysis [3]. With improvements using direct 4-D methods over traditional post-reconstruction analysis often depending on the noise level and with microparameters being noisier than macroparameters, direct 4-D reconstruction methods could potential deliver significantly improved microparametric maps in the body, which could offer additional clinical information compared to macroparametric maps.

In this work we implement a previously proposed direct 4D image reconstruction algorithm, along with a 2-tissue compartment model, to directly estimate for the first time parametric images of microparameters on dynamic abdominal [^{18}F]FDG PET/CT data [4]. The generated parametric maps are also compared with those obtained from traditional post-reconstructed kinetic analysis.

Table. I Kinetic parameters for the different simulated regions.

	K_1 (ml/sec/ml)	k_2 (ml/sec/ml)	k_3 (ml/sec/ml)	bv (ml/ml)
kidney	0.0044	0.0050	0	0.43
spleen	0.0201	0.0318	0.0001	0.25
liver	0.0209	0.0222	0.0001	0.16
pancreas	0.0108	0.0273	0.0004	0.11
heart	0.0033	0.0170	0.0025	0.54
lung	0.0007	0.0048	0.0006	0.15
aorta/ventricles	0	0	0	1
injection site				
soft tissue	0.0008	0.0054	0.0014	0.02
lession1	0.0031	0.0056	0.0023	0.12
lession2	0.0054	0.0111	0.0064	0.16

F. A. Kotasidis is with the Division of Nuclear Medicine and Molecular Imaging, Geneva University Hospital, Geneva, Switzerland and with the Wolfson Molecular Imaging Centre, MAHSC, University of Manchester, UK
J.C. Matthews is with the Wolfson Molecular Imaging Centre, MAHSC, University of Manchester, Manchester, UK
P. M. Price is with the Department of surgery and cancer, Imperial College, London, UK
A.J. Reader is with Montreal Neurological Institute, McGill University, Montreal, Canada
Habib Zaidi is with the Division of Nuclear Medicine, Geneva University Hospital and with Geneva Neuroscience Center, Geneva University, Geneva, Switzerland

II. METHODS

A. Data generation

To evaluate the methods, we used simulated data while a dynamic [^{18}F]FDG PET/CT dataset from a single patient was acquired and considered to evaluate the methods on real datasets. For the simulated data we used a digital body phantom representing 10 major structures in the abdominal and lower thoracic region and 2 lesions embedded in the liver. To generate the time-activity curves (TACs) (28 time frames, [9×10sec, 3×30sec, 4×60sec, 4×120, 8×300sec]), we used a 2 tissue 3 parameter compartment model (K1, k2, k3) with a blood volume component (bv) (4 parameters in total), assuming irreversible kinetics (k4=0). We used typical kinetic parameters similar to those found in the literature, with a population input function taken from real blood data in order for the simulated dataset to be as realistic as possible [5]. The dynamic projection data were generated after forward projecting the image onto a virtual scanner corresponding to the geometry of the Hi-Rez PET/CT and 50 noisy realizations were generated after introducing Poisson noise.

For the real data, a dynamic datasets from a single patient with a mesothelioma in the lung lining was acquired [6]. Whilst on the scanner's bed, the patient was administered with approximately ~400MBq of [^{18}F]FDG and list mode data were acquired over a 62 minute period on the Hi-Rez PET/CT and split in 30 time frames. To generate the input function, late venous sampling was carried out at discrete time points (27min, 47min and 62min) followed by saline flushing, using the samples to scale a population based input function [7].

B. Reconstruction and parameter estimation

The datasets were reconstructed using direct 4D image reconstruction based on a previously proposed algorithm, as well as 3D image reconstruction followed by kinetic analysis. The temporal distribution of the [^{18}F]FDG was modeled in both methods and in both the simulated and patient datasets using a 2-tissue 4 parameter kinetic model, to generate parametric images of K_1, k_2, k_3 and bv. In the simulated dataset the input function used for data generation was also used for parameter estimation and since no delay or dispersion effects were simulated, these effects weren't taken into account during kinetic modeling. However this is not the case on the patient data and delay effects were taken into account during parameter estimation. With the heart ventricles inside the FOV, it is expected that a substantial difference in the tracer arrival time at different body organs/structures located inside the scanned FOV exists. However, fitting for delay, results in having to fit a 5th parameter to noisy data potentially compromising the precision of the kinetic parameters. For that reason a fixed delay throughout the image, common to the post-reconstruction and direct 4-D reconstruction was used. The generalized linear least square method (GLLS) was used to linearize the model and generate the parametric maps.

Initialization of the parameters was performed using average kinetic parameters found in the literature [5].

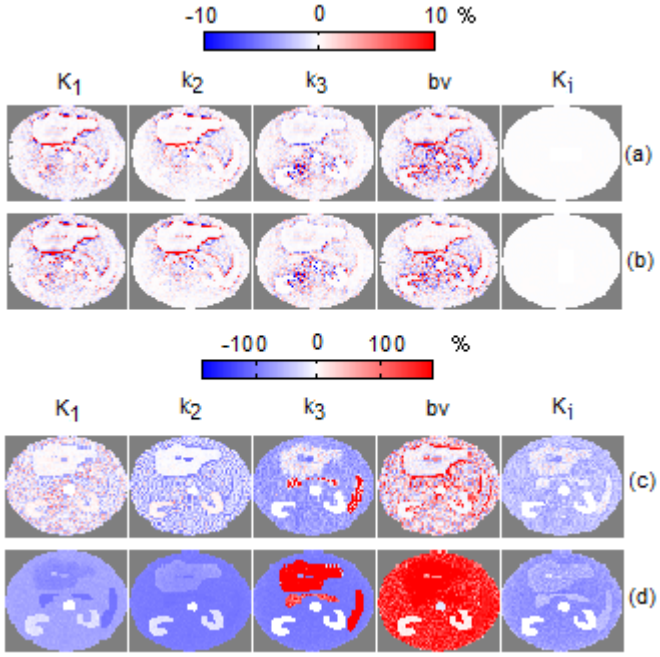

Fig. 1. Bias images for all kinetic parameters (K_1, k_2, k_3, bv and ki) using noiseless (a-b) and noisy (c-d) datasets obtained with direct 4-D reconstruction (a,c) and 3-D reconstruction followed by kinetic analysis (b,d). In the noisy dataset the maps represent the mean voxel wise bias over 50 noisy realizations.

III. RESULTS

A. Simulations

Bias images for K_1, k_2, k_3, bv and K_i are shown in Fig. 1 for the simulated dataset (iteration 15 - subset 21). When noiseless data are considered both the direct (Fig. 1. a) as well as the post-reconstruction methods (Fig. 1. b) give almost identical maps with practically zero bias (small bias at the organ boundaries due to incomplete convergence). When noisy data are considered using the post-reconstruction method, maps with substantial negative bias in K_1 and k_2 are

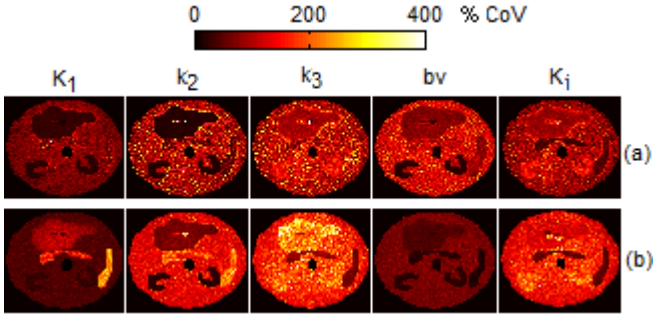

Fig. 2. Coefficient of variation (CoV) images for all kinetic parameters (K_1, k_2, k_3, bv and ki) across the 50 noisy realisations obtained with direct 4-D reconstruction and 3-D reconstruction followed by kinetic analysis.

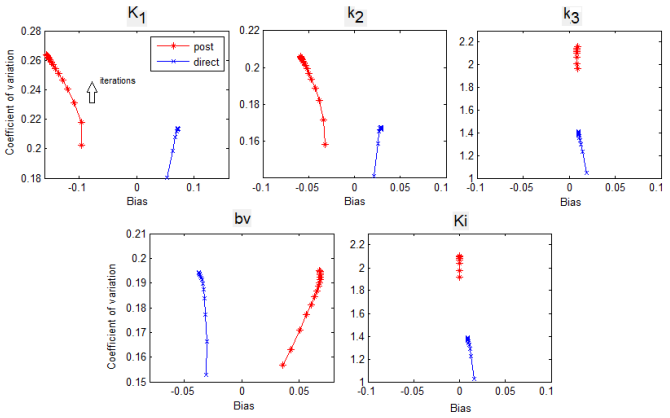

Fig. 3. Plots of bias versus coefficient of variation for all kinetic parameter (K_1, k_2, k_3, bv and Ki) for up to 15 iterations (21 subsets) and for a volume of interest including both left and right kidneys.

obtained (Fig. 1. d), while positive bias is seen in the blood volume. In the k_3 bias image a mixed response is seen with negative bias observed in the soft tissue and the 2 lesions where a relatively high k_3 was simulated compared to the liver, pancreas and spleen where the low simulated k_3 results in a positive bias. Looking at the direct 4D reconstruction (Fig. 1. c), bias in K_1 k_2 and blood volume is massively reduced while in k_3, bias reduction is less dramatic but still noticeable. Although a substantial bias difference is seen in the microparameter maps between the 2 parameter estimation methods this is not as emphatic in the K_i bias maps. This is to be expected, as macroparameters tend to be more robust and less susceptible to noise induced bias.

To assess the variance characteristics of the methods, in Fig. 2 the coefficient of variation parametric maps are shown for all parameters estimated with the direct (Fig. 2. a) and post-reconstruction kinetic analysis (Fig. 2. b) at the 15th iteration (21 subsets). The direct method appears to estimate K_1 and k_2 parameters with reduced variance in almost all organ regions. Looking at the k_3 image a mixed response is seen as in certain regions such as the liver and kidneys, the direct methods exhibits better variance while the opposite is seen in the spleen and pancreas with the post-reconstruction outperforming the direct approach. Similarly in the blood volume, the post-reconstruction shows slightly better variance in the soft tissue (which has a small simulated blood volume). In the rest of the organs both methods exhibit similar variance characteristic. Moving to the K_i, the direct reconstruction outperforms the post reconstruction analysis both in the organ regions as well as the 2 lesions embedded in the liver. Similar to what is seen in the Ki bias images though the variance improvements of the direct method on the macroparameters are not as striking as those seen in the microparameters.

To assess the accuracy and precision of the 2 parameter estimation schemes as a function of iterations, in Fig. 3 bias versus coefficient of variation graphs are plotted for up to 15 iterations for all kinetic parameters, for a region of interest encompassing the whole image volume occupied by the kidneys. In all parameters the direct 4-D reconstruction delivers improvements both in bias and variance, in agreement

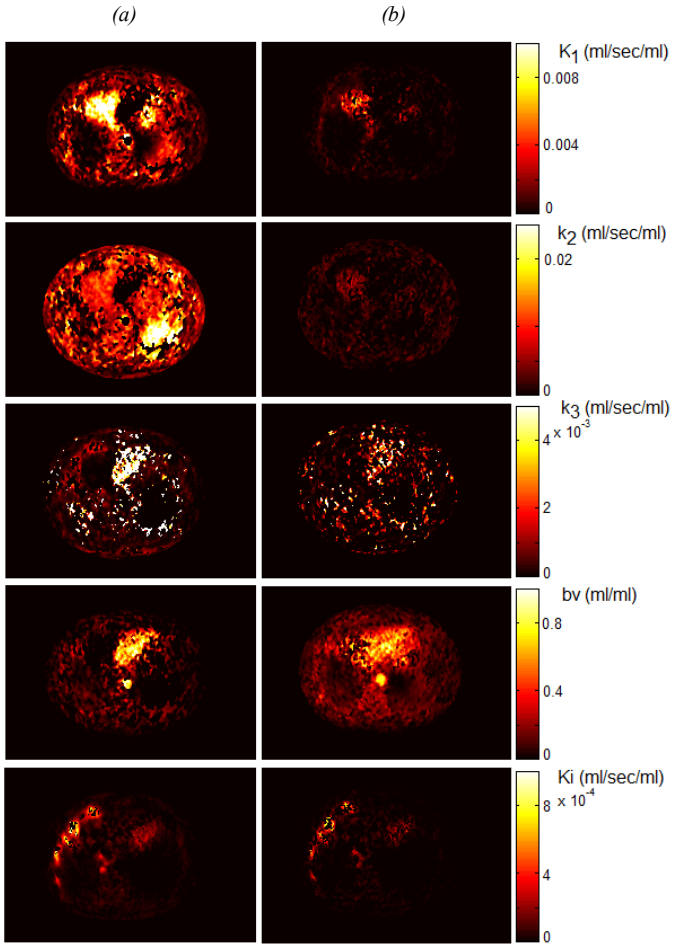

Fig. 4. Parametric images for all kinetic parameters (K_1, k_2, k_3, bv and Ki) obtained with direct 4-D reconstruction (a) and 3-D reconstruction followed (b) by kinetic analysis (4 iterations, 21 subsets) for the clinical dataset. Images of K_1, and k_2 are negatively biased,while blood volume is positively biased using 3D reconstruction compared to the once obtained by 4D reconstruction which follows the trend seen in the simulations. Ki images show quantitative agreement, with the 4D reconstruction being qualitatively better with less variance.

with the improvements seen in the bias and coefficient of variation parametric maps in Fig. 1 and Fig. 2.

B. Clinical dynamic [^{18}F]FDG data

Parametric images of K_1 k_2 k_3, blood volume and K_i estimated with the direct 4-D reconstruction and the post-reconstruction analysis are shown in Fig. 4 for the clinical dataset. The images are shown for a plane traversing the lungs at the base of the myocardium. Looking at the direct method a good separation is seen between the tissue response and the blood volume with the right ventricle being clearly visible in the blood volume image, while the base of the myocardium is visible in the K_1 k_2 and K_i images. Also the beginning of the spleen appears in the K_1 and k_2 images which is not visible in the post-reconstruction parametric maps. Looking at the k_3 image finally the mesothelioma in the lung lining is clearly visible with substantially reduced variance compared to the post-reconstruction k_3 image where the lesion is almost undetected. Similarly the lesion in the direct reconstructed K_i

image, appears also less noisy compared to the post-reconstructed one although the improvements are not as impressive as those observed in k_3. This is in agreement to what observed in the simulated data. Also similar to the simulations, the blood volume image in the post-reconstructed maps appears less noisy but at the same time substantial positively biased compared to the direct image. Although the ground true is not known, this overestimation appears to be absolute as the simulations suggest. Moreover, the myocardium which in the direct method appears correctly in the K_1 and k_2 images, is seen in the blood volume image with post-reconstruction analysis. Looking at the quantitative differences between the methods, in K_1 and k_2, the post-reconstruction maps appear to be substantially underestimated compared to those obtain from the direct method which is in complete agreement with the bias maps from Fig. 1 (c-d). Finally, K_i maps appear to be quantitatively similar between the 2 methods again in accordance to results obtained in the simulations.

IV. Discussion & Conclusion

Recently proposed methods for separation between the tomographic and image based kinetic model problem within a 4D framework allows fast and efficient methods to be used along with non-linear compartmental models to directly estimate constant rates rather than restricting analysis to linear model for estimating macroparamers of interest, such as those obtain from Patlak analysis [4]. In this work for the first time we applied a direct 4D reconstruction algorithm in dynamic [^{18}F]FDG PET/CT body imaging to generate parametric images of microparameters. Data based on simulations as well as patient data suggest that there are substantial gains both in accuracy and precision with reduced bias and variance in parametric maps compared to post reconstruction analysis. In this study we used a 4 parameter model but although challenging, k4 could also be included in the model representing the dephosphorylation constant.

Acknowledgements

This work was supported by the Swiss National Science Foundation under grant SNSF 31003A-135576.

References

[1] A. Rahmim et al Med. Phys. vol. 36, pp. 3654-3670, 2009
[2] F. Kotasidis et al IEEE NSS-MIC Conf. Rec, pp. 2868 – 2874, 2010
[3] A. Rahmim et al, J Nucl. Med, Vol 51, (suppl 2), pp. 354, 2010
[4] J. Matthews et al, IEEE NSS-MIC Conf. Rec, pp. 2435 – 2441, 2010
[5] H.Qiao et al. IEEE/ICME Conf. Rec. pp.154-158, 2011
[6] A. Saleem et al Theranostics vol 1, pp. 290-301, 2011
[7] S Takagi et al. Ann Nucl Med, Vol 18, pp. 297-302, 2004.